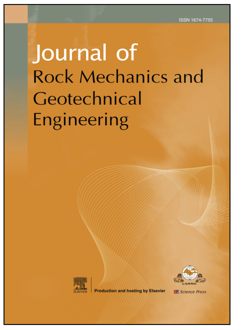

Improvement parameters in dynamic compaction adjacent to the slopes

Elham Ghanbari, Amir Hamidi

PII: S1674-7755(15)00018-9

DOI: 10.1016/j.jrmge.2015.02.002

Reference: JRMGE 135

To appear in: *Journal of Rock Mechanics and Geotechnical Engineering*

Received Date: 9 December 2014

Revised Date: 7 February 2015

Accepted Date: 10 February 2015

ACCEPTED MANUSCRIPT

Journal of Rock Mechanics and Geotechnical Engineering

Journal online: www.rockgeotech.org

Improvement parameters in dynamic compaction adjacent to the slopes

Elham Ghanbari, Amir Hamidi*

School of Engineering, Kharazmi University, Tehran, Iran

Received 9 December 2014; received in revised form 7 February 2015; accepted 10 February 2015

Abstract: Dynamic compaction is a cost-effective method commonly used for improvement of sandy soils. A number of researchers have investigated experimentally and numerically the improvement parameters of soils using dynamic compaction, such as crater depth, improvement depth, and radial improvement, however, these parameters are not studied for improvement adjacent to the slopes or trenches. In this research, four different slopes with different inclinations are modeled numerically using the finite element code ABAQUS, and impact loads of dynamic compaction are applied. The static factors of safety are kept similar for all trenches and determined numerically by application of gravity loads to the slope using strength reduction method (SRM). The analysis focuses on crater depth and improvement region which are compared to the state of flat ground. It can be observed that compacted area adjacent to the slopes is narrower and slightly away from the slope compared to the flat state. Moreover, crater depth increases with increase in slope inclination.

Key words: dynamic compaction; slopes and trenches; crater depth; improvement depth

1. Introduction

Dynamic compaction pioneered by Menard and Broise (1975) has been used for improvement of deep soil layers for decades. In this method, through falling a tamper of 5–30 t from 10–30 m height, improvement depths of 3–9 m are obtained (Lukas, 1995). Soil improvement has been investigated by assessing the experimental tests like standard penetration test (SPT), cone penetration test (CPT) and pressure meter test (PMT) before and after compaction (Mayne et al., 1984; Rollins et al., 1998; Zou et al., 2005; Rollins and Kim, 2010; Zekkos et al., 2013). Also numerical modeling has been performed to investigate soil improvement after compaction (Pan and Selby, 2002; Lee and Gu, 2004; Ghassemi et al., 2010; Mostafa, 2010; Ghanbari and Hamidi, 2014). Dynamic compaction has not been applied near the slopes due to the instability problems. Zou et al. (2005) reported an application of dynamic compaction in placement of a road embankment with 41 m height made of loessial silty clay in China, wherein dynamic compaction was performed at distance of 6 m from the slope heel in soil layers. Few researchers studied the dynamic compaction process near the slopes experimentally (Zhou et al., 2010; Vahidipour, 2014). To the authors' knowledge, there is rare numerical investigation of dynamic compaction near the slopes in the literature. In this study, simulation of dynamic compaction method is performed near the sandy slopes with the same initial factors of safety.

2. Numerical modeling

In this study, two-dimensional (2D) plain strain slope models are used in a finite element code, ABAQUS. Slope models consist of 4 different slope inclinations of 45°, 60°, 75° and 90° with a height of 6 m and appropriate compaction energy of 4000 kN m. Compaction is performed in two steps: the first step is application of gravity load to the whole model in a static manner, and the second one is to apply impact load of the tamper in an implicit dynamic analysis, wherein the tamper is simulated as a rigid body free-falling from a specified height. The latter method was used in previous studies (Pourjenabi et al., 2013; Ghanbari and Hamidi, 2014). In order to keep the similar stability conditions of slopes, the static factors of safety for 4 slope models are kept constant as 1.2, and for this purpose friction angle of soil models is kept to be 30° as a typical value for loose sandy soils and cohesion of soil is changed. Indeed, the soil cohesion has more influence on the factor of safety of the slope, e.g. keeping the factor of safety as 1.2 for 45° and 60° slopes, the soil cohesion changes from 4.5 kPa to 8.0 kPa. Hence the slope model with larger slope inclination should have higher soil cohesion. To determine the static factors of safety in the finite element method (FEM), strength reduction method (SRM) first applied by Matsui and San (1992) is used in this study. In this method, the soil gravity is firstly applied to the whole slope model, and then the soil parameters are reduced gradually by different trial factors of safety to reach the failure. Initial parameters at which slope failure occurs at factor of safety of 1.2 are picked. The onset of failure in slope models is assumed when a sudden increment in nodal displacements is observed. This criterion was used by previous researchers (Griffiths and Lane, 1999; Khosravi and Khabbazian, 2012).

For each slope model, there is a relevant flat model with the same soil properties for comparison. Compaction is simulated for each model at distances of 1–33 m per 4-m interval. Table 1 presents geometry variables of slope models and the compaction energy. Fig. 1 shows definition of slope geometry variables used in numerical analysis, in which x is the tamping distance between tamper edge and slope heel. Lateral and fixed boundaries are also shown in this figure.

Table 1. Geometry variables of slope models and compaction energy.

Height of slope base (m)	Slope height, H (m)	Slope inclination, θ (°)	Compaction energy (kN m)

*Corresponding author. Tel.: +98 21 88830891;
E-mail: hamidi@khu.ac.ir

6	6	45, 60, 75, 90	4000

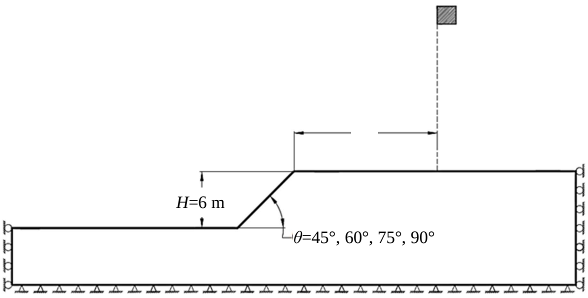

Fig. 1. Slope geometry variables.

The mesh type is quadrilateral 4-noded plain strain elements. The mesh size is finer around the tamper and adjacent to slope with the size of 0.2 m and gradually increases to 1 m at boundaries. Fig. 2 shows mesh type used in the analysis.

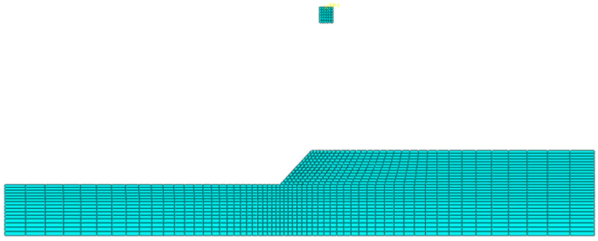

Fig. 2. Mesh type used in numerical analysis.

3. Constitutive model

Cap plasticity model has been used successfully for simulation of dynamic compaction (Thilakasiri et al., 2001; Gu and Lee, 2002; Pak et al., 2005; Ghassemi et al., 2010; Ghanbari and Hamidi, 2014). The model has a number of advantages compared with Mohr-Coulomb model, especially for simulation of compaction phenomenon of soils (Pourjenabi et al., 2013). In this study, the cap plasticity model is used with two yield surfaces, consisting of the fixed yield surface of Drucker-Prager model to indicate shear failure, and the moving caps defining hardening with change in volumetric strains. The yield surfaces are shown in Fig. 3. The fixed and moving yield surfaces for this model can be expressed as follows, respectively:

$$f_1 = \sqrt{J_{2D}} - \alpha J_1 - \kappa = 0 \tag{1}$$

$$f_2 = (J_1 - l)^2 + R^2 J_{2D} - (M - l)^2 = 0 \tag{2}$$

where α and κ are Drucker-Prager constants, J_1 is the first invariant of stress tensor, $\sqrt{J_{2D}}$ is the second invariant of deviatoric stress tensor, l is the coordinate of cap-fixed yield surface intersection on J_1 axis, R is the radius of cap surface in stress space, and M is the hardening parameter of soil depending on plastic volumetric strain (ε_v^p) and initial mean effective stress (M_0). Parameter of R is defined as

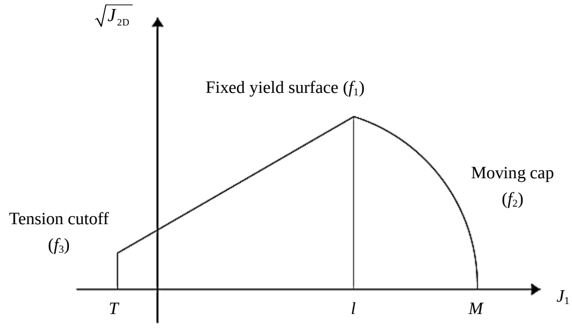

Fig. 3. Yield surface of cap plasticity model in stress space.

$$M = -\frac{1}{D}\ln\left(1 - \frac{\varepsilon_v^p}{w}\right) + M_0 \tag{3}$$

where w and D are the cap plasticity parameters which are dependent on soil compressibility. These parameters were previously calculated by curve fitting with oedometer test results of Oshima and Takada (1997) on a loose sandy soil by Gu and Lee (2002).

As mentioned above, the soil cohesion in each slope model is varied in order to maintain the slope in the same initial factor of safety. The soil cohesions calculated by SRM in finite element are given in Table 2 together with the soil strength parameters and static factors of safety calculated by a limit equilibrium method (LEM). The LEM presented by Morgenstern and Price (1965) has been applied in the program of Geo-Studio software. As it can be seen, the factors of safety obtained by LEM are in good agreement with those obtained by SRM, and the maximum difference is less than 3%.

Table 2. Comparisons of factor of safety by different methods.

H (m)	θ (°)	Cohesion, c (kPa)	Factor of safety	
			SRM	LEM
6	45	4.5	1.2	1.19
6	60	8	1.2	1.19
6	75	13.5	1.2	1.23
6	90	19	1.2	1.24

4. Crater depth results

Fig. 4 shows variation of crater depth versus compaction energy in each blow at different compaction distances from the slope heel. As is observed, the crater depth increases with increase in compaction energy. At the distance of 1 m, the crater depth is higher than that at further distances. As the compaction distance from the slope heel increases, values of crater depth gradually decrease until reaching the values of flat models. It shows that the effects of slopes gradually disappear. Comparing the slope models with different inclinations indicates that the crater depth values at steeper slopes are much higher, also the differences between flat model and slope model at near distances are larger.

5. Relative density contours

Since the total failure has not been observed close to the slope models, the improved region around the slope should be investigated. The contours of relative density in a slope model at distance of 1 m from the slope top and the flat model are shown in Fig. 5. The relative density (D_r) can be obtained by

$$D_r = \frac{e_{max} - e}{e_{max} - e_{min}} \tag{4}$$

where e_{max} and e_{min} are the maximum and minimum void ratios of soil, respectively, obtained from experimental results of Oshima and Takada (1997); and e is the void ratio of soil after compaction, which can be obtained as follows based on volumetric plastic strains produced within the compaction:

$$e = e_0 - (1+e_0)\varepsilon_v^p \tag{5}$$

where e_0 is the initial void ratio.

As it can be seen from Fig. 5, the improved region of flat model consists of relative density contours between 60% and 100% after 10 blows, but at distance of 1 m from the slope top, these contours consist of relative density between 60% and 80% and a small region of 80% to 85%. The improved region close to the slope is narrower and it is not completely created compared to the flat models. Also this region is not symmetric around the tamping point. This behavior has been observed in all slopes with different inclinations. As a result, it can be noticed that, one part of the compaction energy close to slope region increases the soil density and decreases the soil volume, and another part of the energy results in lateral slope displacement which is not appropriate in dynamic compaction operation. Also it can be noted that lateral displacement of slope results in the increase of soil volume and decrease of soil density. As it is clear, the dynamic compaction process is not effective close to the slopes, as it was not applicable before. Thus a distance where the slope stability preserved based on different slope stability criteria must be investigated in further studies. Also different slope geometry and compaction energy should be considered.

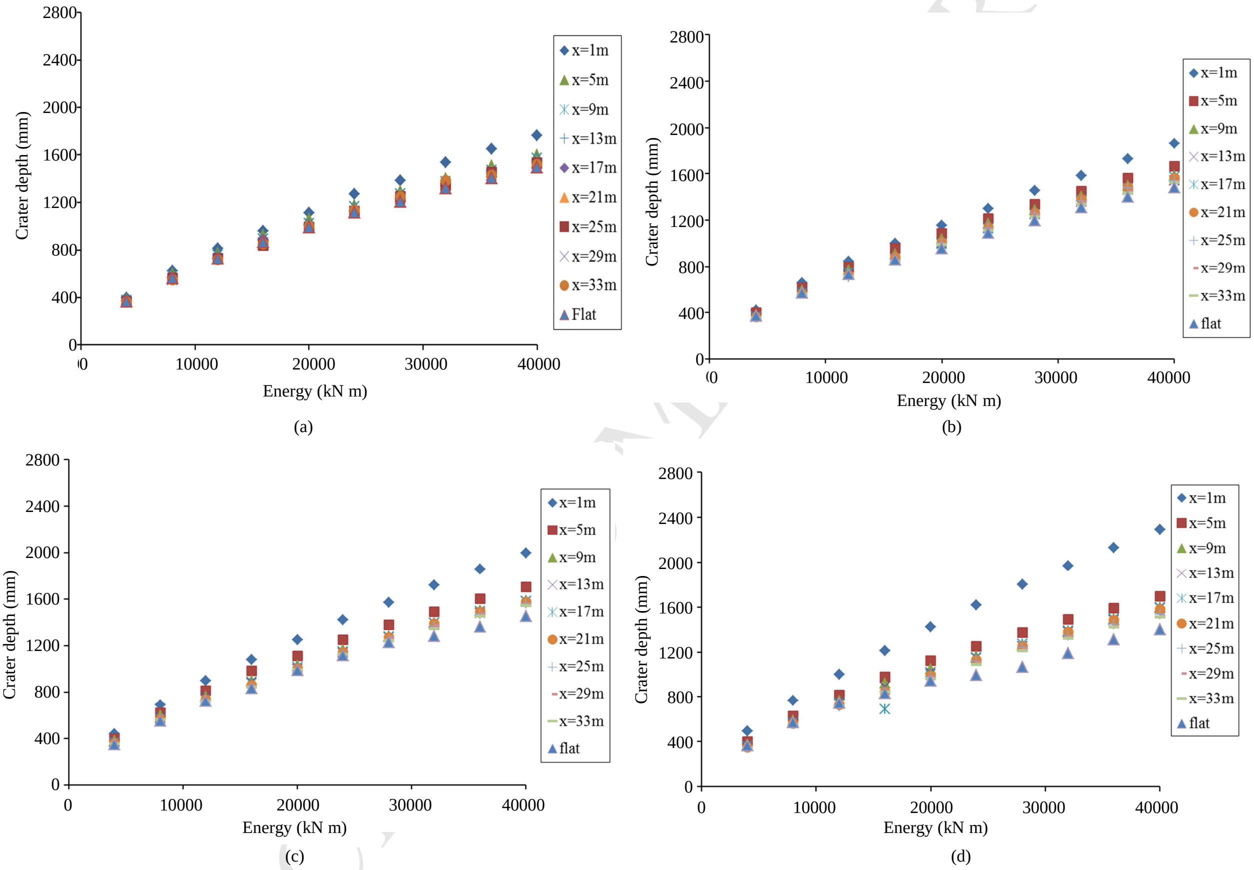

Fig. 4. Results of crater depth values versus compaction energy with different tamping distances at slope inclination of (a) 45°, (b) 60°, (c) 75°, and (d) 90°.

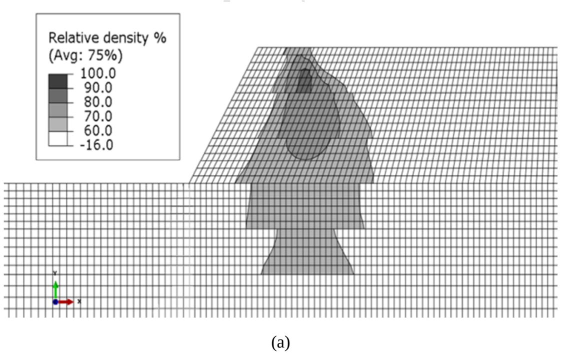

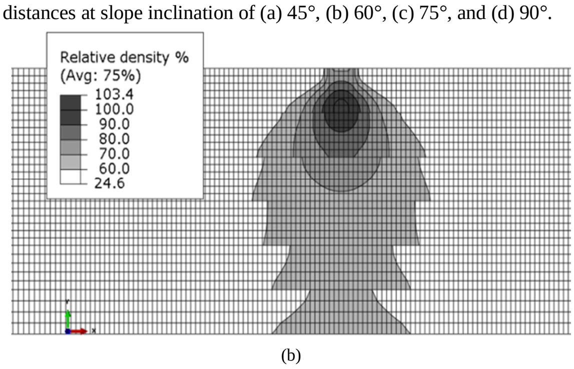

Fig. 5. Results of relative density contours. (a) Slope model; and (b) Flat model.

6. Conclusions

In this study, 2D finite element models are simulated in ABAQUS software to investigate the effects of slope on dynamic compaction parameters. By using SRM and applying gravity to the whole slope, the static factors of safety of all models were kept at 1.2. The factor of safety calculated by LEM was in good agreement with Morgenstern-Price method. After tamping of 10 blow counts adjacent to the slope heel, when compared with flat models, the following results can be drawn:

(1) At near distances of compaction from the slope heel, crater depth values are much higher than those at far distances. As the distance from slope heel increases, crater depth values approach to the values in flat models.
(2) It is observed that in steeper slopes, crater depth values become higher. Also, a great difference between the values of flat models and slope models at near distances is observed clearly.
(3) Comparing the relative density contours at distance of 1 m from slope heel and flat model, it can be seen that the contours are not created completely and the improved region is narrower. At distance of 11 m, only a small region of 80% to 85% relative density is created, whereas at flat models these contours appropriately reach 100%. As a result, dynamic compaction is not effective adjacent to the slopes. Hence for determining a safe distance from slope heel, more investigations shall be performed and different slope stability criteria shall be considered.

Conflict of interest

The authors wish to confirm that there are no known conflicts of interest associated with this publication and there has been no significant financial support for this work that could have influenced its outcome.

References

Ghanbari E, Hamidi A. Numerical modeling of rapid impact compaction in loose sands. Geomechanics and Engineering 2014; 6(5): 487-502.

Ghassemi A, Pak A, Shahir H. Numerical study of the coupled hydro-mechanical effects in dynamic compaction of saturated granular soils. Computers and Geotechnics 2010; 37(1-2): 10-24.

Griffiths DV, Lane PA. Slope stability analysis by finite elements. Geotechnique 1999; 49(3): 387-403.

Gu Q, Lee FH. Ground response to dynamic compaction. Geotechnique 2002; 52(7): 481-93.

Khosravi M, Khabbazian M. Presentation of critical failure surface of slopes based on the finite element technique. In: Proceedings of GeoCongress: State of the Art and Practice in Geotechnical Engineering. Reston, Virginia, USA: American Society of Civil Engineers; 2012. pp. 536-45.

Lee FH, Gu Q. Method for estimating dynamic compaction effect on sand. Journal of Geotechnical and Geoenvironmental Engineering 2004; 130(2): 139-52.

Lukas RG. Geotechnical engineering circular No. 1 – Dynamic compaction. Publication No. FHWA-SA-95-037, 1995.

Matsui T, San KC. Finite element slope stability analysis by shear strength reduction technique. Soils and Foundations 1992; 32(1): 59-70.

Mayne PW, Jones JS, Dumas JC. Ground response to dynamic compaction. Journal of Geotechnical Engineering 1984; 110(6): 757-774.

Menard L, Broise Y. Theoretical and practical aspects of dynamic consolidation. Geotechnique 1975; 25(1): 3-16.

Morgenstern NR, Price VE. The analysis of the stability of general slip surfaces. Geotechnique 1965; 15(1): 79-93.

Mostafa K. Numerical modeling of dynamic compaction in cohesive soils. PhD Thesis. Akron, OH, USA: University of Akron, 2010.

Oshima A, Takada N. Relation between compacted area and ram momentum by heavy tamping. In: Proceedings of the 14th International Conference on Soil Mechanics and Foundation Engineering (ICSMFE). Rotterdam, Netherland: A.A. Balkema; 1997. pp. 1641-4.

Pak A, Shahir H, Ghassemi A. Behavior of dry and saturated soils under impact load during dynamic compaction. In: Proceedings of the 16th International Conference on Soil Mechanics and Geotechnical Engineering (ICSMGE). Rotterdam, Netherland: Millpress Science Publishers; 2005. pp. 1245-8.

Pan JL, Selby AR. Simulation of dynamic compaction of loose granular soils. Advances in Engineering Software 2002; 33(7-10): 631-40.

Pourjenabi M, Ghanbari E, Hamidi A. Numerical modeling of dynamic compaction in dry sand using different constitutive models. In: Proceedings of the 4th ECCOMAS Conference on Computational Methods in Structural Dynamics and Earthquake Engineering, Kos Island, Greece, 2013.

Rollins KM, Jorgensen SJ, Ross TE. Optimum moisture content for dynamic compaction of collapsible soils. Journal of Geotechnical and Geoenvironmental Engineering 1998; 124(8): 699-708.

Rollins KM, Kim J. Dynamic compaction of collapsible soils based on U.S. case histories. Geotechnical and Geoenvironmental Engineering 2010; 136(9): 1178-86.

Thilakasiri HS, Gunaratne M, Mullins G, Stinnette P, Kuo C. Implementation aid for dynamic replacement of organic soils with sand. Journal of Geotechnical and Geoenvironmental Engineering 2001; 127(1): 25-35.

Vahidipour A. Experimental study of dynamic compaction adjacent to the slope. MS Thesis. Tehran, Iran: Kharazmi University, 2014.

Zekkos D, Kabalan M, Flanagan M. Lessons learned from case histories of dynamic compaction at municipal solid waste sites. Journal of Geotechnical and Geoenvironmental Engineering 2013; 139(5): 735-51.

Zhou Z, Chao WL, Liu BC. Model test study on dynamic responses of step-shaped loess slope with dynamic compaction. In: Proceedings of the 10th International Conference of Chinese Transportation Professionals. Reston, VA, USA: American Society of Civil Engineers; 2010. pp. 3227-37.

Zou WL, Wang Z, Yao ZF. Effect of dynamic compaction on placement of high-road embankment. Performance of Constructed Facilities 2005; 19(4): 316-23.

Amir Hamidi is an Associate Professor in the School of Engineering at Kharazmi University of Tehran since 2006. He has obtained his B.Sc. and M.Sc. degrees from Civil Engineering Department of Sharif University of Technology in 1997 and 1999, respectively. He has also received his Ph.D. degree in Geotechnical Engineering from Department of Civil Engineering, Sharif University of Technology in 2005 working on experimental behavior and constitutive modeling of cemented gravely sands. His research interests include experimental soil mechanics, plasticity concepts and constitutive modeling and ground improvement. Dr. Hamidi has been professionally working in a variety of ground improvement projects especially dynamic compaction and land reclamation.